Industrial Crops and Products 58 (2014) 305–314

Contents lists available at ScienceDirect

Industrial Crops and Products

journal homepage: www.elsevier.com/locate/indcrop

Cassava (*Manihot esculenta*) starch films reinforced with natural fibrous filler

Florencia Versino, María Alejandra García*

CIDCA (Centro de Investigación y Desarrollo en Criotecnología de Alimentos), Facultad de Ciencias Exactas, Universidad Nacional de La Plata–Centro Científico Tecnológico La Plata (CCT-La Plata) CONICET, 47 y 116 S/N°, La Plata (B1900AJJ), Buenos Aires, Argentina

ARTICLE INFO

Article history:
Received 27 December 2013
Received in revised form 14 April 2014
Accepted 15 April 2014

Keywords:
Eco-compatible materials
Cassava starch films
Natural fillers
Optical properties
Water vapor permeability
Mechanical properties

ABSTRACT

The remaining fibrous residue of cassava starch extraction was characterized and used as film filler in order to obtain an enhanced fully biodegradable starch-based composite. Film-forming gelatinized cassava starch suspensions increased significantly their apparent viscosity and storage modulus with filler addition, although no segregation of filler particles was observed. Homogenous films were obtained from 3% w/w cassava starch film-forming suspensions including glycerol as plasticizer and the remaining fibrous residue. Plasticizer concentration was optimized in reinforced starch films. SEM micrographs evidenced that the filler was structurally incorporated in the matrix, although concentrations of 3% led to more heterogeneous surfaces because of the presence of large size filler particles. Reinforced films exhibited UV-barrier capacity and adequate water vapor barrier properties ($14.6 \pm 0.7\ 10^{-11}$ g/m s Pa) and tensile strength (18.01 ± 0.19 MPa) when 25% w/w glycerol was added as plasticizer. Filler addition reinforced the starch matrix increasing its mechanical resistance: 1.5% residue content increased over 900% the films elastic modulus. Furthermore, the obtained eco-compatible materials could be heat sealed, which indicates their suitability for packaging development. In conclusion, an integral approach to cassava roots use has been proposed, expanding its scope and providing added value to the remaining residue of starch extraction.

1. Introduction

Interest in biodegradable films development from renewable sources is growing due to increased environmental awareness. Among natural polymers, starch has been considered as one of the most promising materials because of the attractive combination of availability, price and performance (Abdillahi et al., 2013; López and García, 2012). Cassava (*Manihot esculenta*), in particular, is an important starch source in some countries like Brazil, which is the largest cassava-producing country (Leonel et al., 2003), as well as in Thailand, Malaysia, Indonesia and some regions of Africa (United Nations Conference on Trade and Development, 2012). Besides, the use of cassava starch for film formulation has been extensively studied (Famá et al., 2006, 2007; Mali et al., 2005; Prakash Maran et al., 2013). In previous works a procedure for starch extraction from tuberous roots like ahipa (*Pachyrhizus ahipa*) and cassava was developed and optimized (López and García, 2012; López et al., 2010).

In recent years, the use of natural fibers as reinforcing materials in polymers and composites has attracted much attention. Compared to inorganic fillers, the main advantages of lignocellulosics are their renewable nature, biodegradability, low energy consumption, wide variety available throughout the world, low cost and density, as well as high specific strength and modulus (Bodirlau et al., 2013; Castillo et al., 2013; Gilfillan et al., 2012; Satyanarayana et al., 2009). Furthermore, they present high sound attenuation, and comparatively easy processing due to their flexibility and non-abrasive nature which allow high filling levels (Al-Oqla and Sapuan, 2014; Shalwan and Yousif, 2013). In spite of these desirable properties, lignocellulosic fillers are used only to a limited extent in industrial practices, mainly due to difficulties associated with surface interaction in the case of synthetic polymers (Satyanarayana et al., 2009; Shalwan and Yousif, 2013).

Natural fibers can be obtained from agro-industrial or agricultural residues, providing added value to raw materials. Starch composites with different cellulose fibers have been discussed and reviewed including, among others, wood and kenaf fibers (Kuciel and Liber-Knec, 2009), softwood short fibers (Müller et al.,

* Corresponding author. Tel.: +54 221 4254853; fax: +54 221 4254853/+54 221 4249287.
E-mail addresses: magarcia@quimica.unlp.edu.ar, malegarcia09@gmail.com (M.A. García).

http://dx.doi.org/10.1016/j.indcrop.2014.04.040
0926-6690/

2009), pehuen cellulosic husk (Castaño et al., 2012), pulp aspen fiber (Konar et al., 2013) and date palm and flax fibers (Ibrahim et al., 2014). Likewise, lignocelluloseic fillers have been added to other biodegradable and synthetic materials. Behera et al. (2012) reported the inclusion of jute fibers in a soy protein matrix and Ludueña et al. (2012) have reinforced polycaprolactone films with cotton fibers to enhance film properties.

To the best of our knowledge there are no reports about films reinforced with the residue remaining from starch extraction. Thus, residue chemical composition as well as SEM morphology should be studied in relation to its reinforcing capacity as well as the properties of the obtained materials containing this natural filler. This is an innovative and interesting application to revalorize and add value to this industrial waste, with the consequent diminution of waste volumes.

The aim of the present work was to develop and characterize eco-compatible plasticized films based on cassava starch and the residue remaining from starch extraction as filler reinforcing material, proposing an integral approach of the whole tuber root.

2. Materials and methods

2.1. Materials

Manihot esculenta (cassava) roots were provided by the INTA Montecarlo Experimental Station farm (Misiones, Argentina; 26°33′40.15″ Latitude South and 54°40′20.06″ Longitude West). Starch was then extracted from the roots following the procedure described by López et al. (2010). The fibrous residual paste obtained from such process was dried, ground and sieved to be used as filling material.

2.2. Fibrous residue characterization

2.2.1. Scanning electron microscopy (SEM)

Microstructure and morphology of dry milled and sieved fibrous residue were studied by SEM, JEOL JSM 6360 (Japan). Samples were mounted on bronze stubs using a double-sided tape and coated with a gold layer (40–50 nm), all samples were analyzed using an accelerating voltage of 20 kV, under high vacuum mode.

2.2.2. Dry matter and total ash content

Residual water content was gravimetrically quantified by placing residue samples in an oven (GMX 9203A PEET LAB, USA) at 105 °C until reaching constant weight. Results were expressed as percentage (%) of the initial weight. Total ash quantification was also performed gravimetrically after incineration in a muffle furnace (Indef 331, Argentina) at 550 °C. The percentage (%) of total ash on a dry basis was then calculated.

2.2.3. Lipid fraction

Residue samples (12 g) were extracted in a Soxhlet apparatus with hexane. The residue obtained in the flask after solvent recovery and evaporation (total fat) was weighed. Results were expressed as percentage (%) on dry basis.

2.2.4. Crude protein

Fibrous residue samples (1 g) were analyzed for total nitrogen content by AOAC 984.13 Kjeldahl method (1990). Results were expressed as percentage (%) on dry basis.

2.2.5. Total dietary fiber (TDF)

The content of TDF in the cassava residue was measured by the enzymatic kit K-TDFR 05/12 Megazyme© (Ireland) following AOAC 985.29 method (1997). Results were expressed as percentage (%) on dry basis.

2.2.6. Lignin content

Klason lignin content was determined following the TAPPI T222om-11 method (2011), which is based on the isolation of lignin after polysaccharide hydrolysis by concentrated sulfuric acid (72%) treatment. Fibrous residue samples (2 g) were macerated using 72% H_2SO_4 (40 ml) at room temperature and kept under such conditions for 2 h. Acid solution was later diluted with distilled to 3% concentration and the system was later kept under boiling conditions with reflux for 4 h. The acid-insoluble lignin content was calculated gravimetrically, considering the filtered dried solid remaining. The Klason soluble lignin was determined by absorbance values at 280 and 215 nm from the remaining solution as was described by (Guimarães et al., 2009). Results were expressed as percentage (%) on dry basis.

2.2.7. Particle size distribution

Filler particle size distribution was studied using a laboratory test sieves (ALEIN International, Argentina) with the following set of ASTM standard meshes: 500, 425, 355, 300, 250, 212, 180, 150, 106, 75 and 53 μm. The sieving procedure was done for 100 g of residue during 10 min. The fractions retained in each mesh were separated and weighed. The fractionation process was performed in duplicate.

2.3. Film-forming suspensions: preparation and characterization

Aqueous suspensions of 3% w/w starch with different fibrous filler contents (0–3% w/w) were gelatinized at 90 °C during 20 min. Glycerol (Anedra, India) was added as plasticizer to gelatinized suspensions at concentrations varying from 0 to 35 g/100 g of starch.

Film formulation nomenclature used was: F to indicate de fiber content in weight percentage, NG for non-plasticized films and G for films plasticized with 25% of glycerol with respect to the starch content. Nomenclature used is summarized in Table 1.

The rheological characterization of film-forming suspensions was performed in a Rheo Stress 600 ThermoHaake (Haake, Germany) rheometer using a plate–plate system PP35 (1 mm gap) at controlled temperature (25 °C). Rotational mode was used to investigate flux behavior of starch gelatinized suspensions, plotting shear stress (τ) versus shear rate ($\dot{\gamma}$). The resulting curves were mathematically modeled as Ostwald de Waele fluids according to the following equation:

$$\tau = k \times \dot{\gamma}^n \quad (1)$$

where k is the consistency coefficient and n the flow behavior index. The apparent viscosity of non-newtonian film-forming suspensions was calculated at 500 s^{-1}. To evaluate the time dependence of these systems, the corresponding thixotropic or anti-thixotropic indexes were determined. Thixotropic and rheopectic (anti-thixotropic) materials exhibit, respectively, decreasing and increasing shear stress (and apparent viscosity) over time at a fixed rate of shear

Table 1
Film composition and nomenclature used.

Film composition		Nomenclature
Fiber (%)	Glycerol (%)	
0	0	0FNG
0	25	0FG
0.75	25	0.75FG
1.5	0	1.5FNG
1.5	25	1.5FG
3	25	3FG

(Steffe, 1996). These indexes were calculated as the area between the flux curves, taking positive values for thixotropic systems and negative for anti-thixotropic ones.

Viscoelastic behavior of gelatinized starch suspensions was studied by performing dynamic assays. The linear viscoelasticity range was determined in a stress sweep (0–30 Pa) assay at constant frequency (1 Hz). Then, frequency sweeps (0.01–100 Hz) were performed at constant stress. The dynamic rheological parameters recorded were the storage modulus (G') and the loss modulus (G''). These parameters were measured on the gelatinized starch suspensions and after 24 h and 48 h, in order to evaluate the storage time effect. The tangent of the phase angle ($\tan \delta = G''/G'$) and the complex shear stress (G^*) were also acquired. Mechanical spectra were obtained by plotting G' and G'' versus frequency (ω).

2.4. Film forming capacity

To evaluate the film forming capacity of cassava starch with different fiber contents, approximately 20 g of film-forming suspensions were cast onto Petri dishes (diameter 8.7 cm). After drying in a ventilated oven (GMX 9203A PEET LAB, Argentina) at 50 °C for 4 h, films were removed from the plates and stored at 20 °C and 65% relative humidity (RH) for at least 48 h. Homogeneity and appearance of the films were examined as well as the film removal easiness. Film properties were measured on conditioned films.

2.5. Film properties

Thickness of the films was evaluated using a digital coating thickness gauge Check Line DCN-900 (New York, USA) for non-conductive materials on non-ferrous substrates. Ten measurements were randomly taken at different locations for each specimen and the mean value was reported.

Humidity content was determined by measuring the weight loss of films, upon drying in an oven at 105 °C until constant weight. Samples were analyzed at least in triplicate and results were expressed as percentage (%) of moisture content of samples.

Homogeneity and appearance of the films were examined by visual observation and scanning electron microscopy (SEM) with a JEOL JSM 6360 electron microscope (Japan). For cross-section observations films were cryofractured by immersion in liquid nitrogen. Film pieces were mounted on bronze stubs using a double-sided tape and coated with a gold layer (40–50 nm), enabling surface and cross-section visualization. All samples were analyzed using an accelerating voltage of 20 kV, under high vacuum mode.

To evaluate UV barrier film capacity the absorbance spectrum (200–800 nm) was recorded using a U-1900 spectrophotometer (HITACHI, Japan). Films were cut into rectangles (3 cm × 1 cm) and placed on the internal side of a quartz spectrophotometer cell. Film opacity (AU nm) was defined as the area under the recorded curve determined by an integration procedure according to Castillo et al. (2013) and the standard test method for haze and luminous transmittance of transparent plastics recommendations ASTM D1003-00 (2000).

Films color was evaluated using a Minolta colorimeter CR 400 Series (Konica Minolta Sensing Inc., Osaka, Japan) calibrated with a standard ($Y = 93.2$, $x = 0.3133$, $y = 0.3192$). The CIELab scale was used, luminosity (L) and chromatic parameters a* (red–green) and b* (yellow–blue) were measured. The functions *hue angle* [$h^\circ = \tan^{-1}$ (b*/a*)] and *Chroma* [$C^* = (a^{*2} + b^{*2})^{1/2}$] were calculated. Color assays were performed by placing the film samples over the standard. Samples were analyzed in triplicates, recording five measurements at different positions for each sample.

Water vapor permeability (WVP) tests were conducted using ASTM method E96 (1996) with several modifications according to (López et al., 2008). After steady-state condition was reached, the acrylic permeation cells were weighed (0.0001 g) at initial time and at 1 h interval over 8 h. The WVP (g/m s Pa) was calculated considering the thickness of each tested film, as well as the cell area and the water vapor partial pressure difference across the film at 20 °C.

Mechanical profiles (stress–strain curves) were obtained using a texturometer TA.XT2i-Stable Micro Systems (England) with a tension grip system A/TG. Probes of 6 cm in length and 0.7 cm in width were cut. At least 10 probes were tested for each film formulation. Tensile strength (TS, MPa) and elongation at break (E, %) were calculated as described by López et al. (2011). Toughness (J) is defined as the amount of energy that a film absorbs before yielding. This is an important parameter which was obtained from the area under the stress–strain curve using the Origin 8 software (Origin-Lab Corporation, Northampton, MA).

Dynamic mechanical analyses (DMA) were conducted in a Q800 (TA Instruments, New Castle, USA) equipment with a liquid N_2 cooling system, using a clamp tension and rectangular film probes (length: 30 mm, width: 6 mm and thickness: determined as described previously). The elastic modulus (Young's modulus, MPa) of samples with different fibrous filler content was determined by mathematical modeling of stress–strain curves obtained by DMA, in accordance with model used by Chillo et al. (2008).

$$\sigma_T = E_c \times \varepsilon_T \times e^{(-\varepsilon_T \times K)} \quad (2)$$

where ε_T and σ_T are the true strain and the true stress, respectively, calculated according to (Mancini et al., 1999); E_c is the elastic modulus (i.e. the tangent to the stress strain curve at the origin); and K is a constant value, regarded as a fitting parameter.

The heat-sealing properties of the films were measured and compared with that of synthetic low density polyethylene (CRYOVAC® PD-941). Films with 1.5% fiber content and plasticized with 0.75% glycerol were sealed and tested in the texturometer previously described as detailed by López et al. (2011). The heat seals were produced using an impulse-wire thermosealer (HermePlas, Argentina) on pieces of films of 8.7 cm of diameter. This equipment works at 220 V leading to a fixed temperature of 154.3 ± 8.5 °C, which was measured using a K-type thermocouple connected to a data logger thermometer (TES-1307, Taiwan). The optimum sealing-time that resulted in the best zip quality was 1.84 ± 0.01 s.

Mechanical patterns were registered and failure modes were determined according to ASTM standard method F88-00 (2001).

2.6. Statistical analysis

All experiments were performed at least in duplicates, with individually prepared and casted films as replicated experimental units as described previously in each determination. Systat-software (SYSTAT, Inc., Evanston, IL, USA) version 10.0 was used for multifactor analysis of variance. Differences in the properties of the films were determined by Fisher's least significant difference (LSD) mean discrimination test, using a significance level of $\alpha = 0.05$.

3. Results and discussion

3.1. Extraction and characterization of fibrous residue filler

Pulp obtained as a residue from cassava roots starch extraction, following the method described by López et al. (2010), was dried in oven at 50 °C up to constant weight. The fibrous residue yield was 36.13 ± 1.07% w/w. Then, it was ground to smaller pieces and sieved with 500 μm mesh, in order to have a bounded particle maximum size. The fibrous residue presented a heterogeneous particle size distribution (Fig. 1a), resulting 44% of the particles bigger than 53 μm.

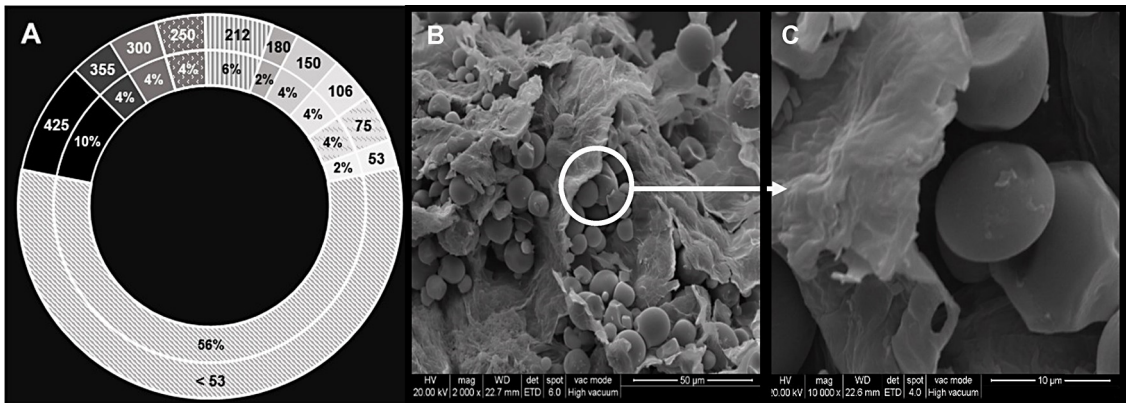

Fig. 1. Fibrous cassava residue characterization: (a) particle size distribution of fibrous cassava residue; (b) scanning electronic microscopy (SEM) micrographs of fibrous cassava residue 500× and (c) 2000×.

The chemical composition of the residue is shown in Table 2; being carbohydrates, mainly starch, the principal component. Two different techniques were used to characterize the fibrous fraction of the residue. Total dietary fiber (TDF) and lignin content assays were performed taking into consideration that the fibrous residue derives from an edible root, in order to determine the portion of the residue that acts as dietary fiber. The lignin content was determined in order to evaluate the resistant components proportion of the fibrous residue, which also contributes in a major degree to the reinforcement of the films.

The SEM morphological characterization of the fibrous residue is shown in Fig. 1b and c, where the starch granules surrounded by the remaining cell walls of the parenchyma tissue can be observed. Identified starch granules exhibited both round and polygonal shapes, differences observed are attributed to the bimodal granule size distribution of cassava starch (Doporto et al., 2012).

3.2. Characterization of film-forming suspension

Rheological behavior of film-forming starch suspensions determines the processing conditions needed to obtain films at industrial scale. Besides, rheological properties are related with the presence of some defects (bubbles and pores) in polymeric matrixes (Han and Gennadios, 2005). In this sense, rotational assays allowed us to analyze starch pastes rheological behavior when they are submitted under conditions close to industrial processing parameters such as high shear stress. Fig. 2 shows flow curves corresponding to gelatinized starch-suspensions without glycerol or fiber, and those plasticized with 25% glycerol and different fiber concentrations. All of them presented a pseudoplastic behavior ($n < 1$), which was satisfactorily adjusted by Ostwald de Waele model. In addition, all samples were characterized as thixotropic, indicating that the rheological behavior of these systems was time dependent (Fig. 2). Thixotropic materials exhibit decreasing shear stress and apparent viscosity over time at a fixed shear rate, due to the networks structure break down (Steffe, 1996). The corresponding

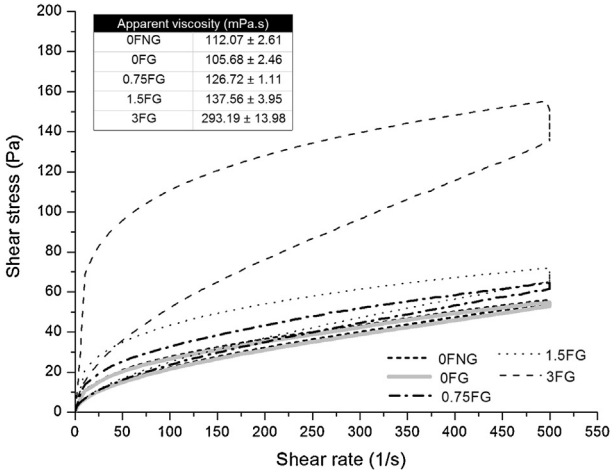

Fig. 2. Flow curves and apparent viscosities at 500 s^{-1} of film-forming cassava starch suspensions: (·····) 0FNG; (——) 0FG; (–·–) 0.75FG; (·····) 1.5FG and (– –) 3FG.

thixotropic indexes were calculated as the area between the flux curves, being 1977.5 and 1774 Pa/s for starch suspensions without filler, with and without plasticizer respectively; while for suspensions with increasing concentration of filler the indexes resulted higher: 3929.5, 7683.5 and 25515 Pa/s for 0.75%, 1.5% and 3% fiber content. The difference in thixotropic indexes for samples without filler plasticized and not plasticized was not significant ($p > 0.05$), whereas such differences resulted significant ($p < 0.05$) for samples with varying content of filler. Filler particles promote structural defects favoring the breakdown of the network when submitted at high shear rate.

From the rotational assays it was also observed that with the inclusion of the filler in suspensions apparent viscosity at 500 s^{-1} increased significantly ($p < 0.05$), as shown in Fig. 2.

Table 2
Chemical composition (% w/w) of the fibrous residue remaining from cassava starch extraction.

Fiber			Carbohydrates[a]	Lipids	Protein	Humidity	Ashes
Total dietary fiber	Klason lignin						
	Acid insoluble	Acid soluble					
4.2 ± 2.8	1.21 ± 0.57	0.41 ± 0.01	82.57 ± 1.28	0.17 ± 0.015	1.25 ± 0.01	10.56 ± 1.58	0.86 ± 0.04

Note: Reported values correspond to the mean ± standard deviation. Results are expressed on dry basis.
[a] Carbohydrates were calculated as the mathematical difference from the total mass.

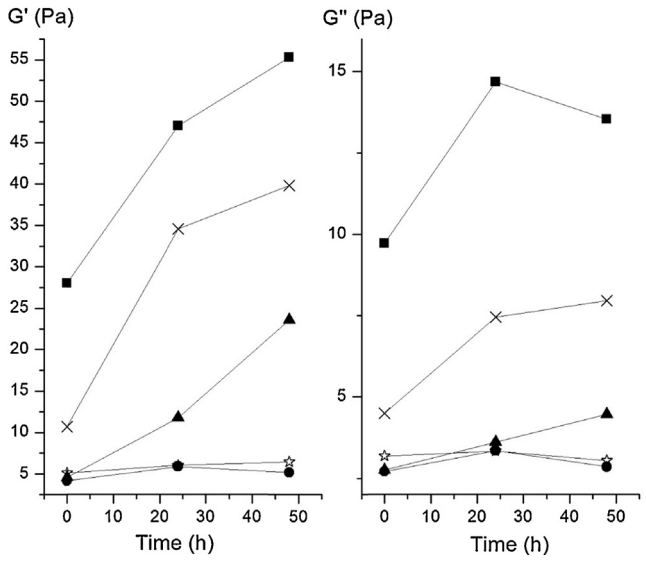

Fig. 3. Variation of storage module (G') and loss module (G'') with storage time: (–☆–) 0FNG; (–●–) 0FG; (–▲–) 0.75FG; (–×–) 1.5FG and (–■–) 3FG.

Oscillatory assays evaluated viscoelastic behavior of gelatinized starch film-forming suspensions within linear viscoelasticity range where samples do not suffer structural damage. From stress sweeps it was determined that the linear viscoelasticity range was extended up to 1.4 Pa or more for all starch pastes, so for frequency sweeps 1 Pa was the shear stress value selected. It is well known that starch paste retrogradation is a time dependent phenomenon that could affect the stability of film-forming suspensions. Fig. 3 shows the variation of storage module (G') and loss module (G'') with storage time for all formulations tested. In all samples G' values resulted significantly higher ($p < 0.05$) than G'' ones, remained practically constant throughout all the frequency range analyzed, behaving like a weak gel. G' and G'' values for cassava starch gelatinized suspensions increased with the addition of fibrous filler and with storage time. Although the firmness of the pastes increases, no segregation was observed confirming that the filler particles remained suspended. These results are critical and should be considered in scaling up the process.

When glycerol was incorporated to starch matrixes both G' and G'' decreased; however the tendency of the curves resulted similar to those corresponding to unplasticized films (Fig. 3). Similar trend was reported by other authors working on starch based film-forming suspensions plasticized with different polyols and sugars (Muscat et al., 2012; Rodriguez-Gonzalez et al., 2004; Zhang et al., 2013).

These results are in agreement with the apparent viscosities observed at 500 s^{-1} shear rate. For samples without fiber the addition of plasticizer lowered the apparent viscosity from 112 mPa s to 105 mPa s, whereas the incorporation of 0.75, 1.5 and 3% w/w of filler increased the parameter in 20, 30 and 177%, respectively.

3.3. Cassava starch film physicochemical properties

Cassava film-forming suspensions required an additional bubble removal step under vacuum, due to their high apparent viscosity, since bubbles conditioned the appearance of pores as well as other defects on films surface during drying process. This procedure was also applied by Perdomo et al. (2009) working on cassava starch polymeric matrix development. All degassed formulations tested could form continuous films, which were easily removed from the molds.

Cassava starch films exhibited thickness values around 67 μm, glycerol addition reduced the films thickness to 48 μm. Film thickness comparison with those reported for hydrocolloid-based films is difficult because casting ratio used is generally omitted. On the other hand, the incorporation of the filler derived in significantly thicker and rougher films, with thickness proximate to 140 μm for 1.5% fiber content films. Such an effect, as well as the high standard deviation associated (Table 3), was attributed to the presence of large size filler particles within the polymer matrix, as shown in Fig. 1a.

Films humidity was significantly ($p < 0.05$) affected by both glycerol and fiber addition. As could be expected, humidity content of plasticized films was higher than that of unplasticized ones, due to the hydrophilic character of glycerol. The plasticizer effect on hydrocolloid-based films has been extensively described in the literature (Sothornvit and Krochta, 2005) based on the promotion of chemical interactions, molecular mobility and free volume increase (Mali et al., 2005). Meanwhile, an increase in filler content resulted in lower moisture content of reinforced films.

SEM was used to examine the microstructure and the interfacial adhesion of cassava starch and its reinforced biocomposites. Fig. 4 shows SEM micrographs of the cryofractured surfaces of plasticized films based on cassava starch. Plasticized cassava starch films showed homogeneous surfaces and compact structures (Fig. 4a). The addition of the filler led to the formation of films with more heterogeneous surfaces where large size particles of the reinforcing material covered by the starch matrix can be observed (Fig. 4b and c). This discontinuity was also evident in thickness measurements, which presented greater dispersion for reinforced samples (Table 3). The fact that fibers were coated with the starch matrix indicated that the residue was structurally incorporated in the network (Fig. 4b and c), owing this to a high compatibility between both components. Good adhesion between the filler and the matrix leads to a resistant interface (Kuciel and Liber-Knec, 2009), consequently reinforcing the matrix enhancing their mechanical resistance. Similar observations have been reported by other authors for starch based composites (Ibrahim et al., 2014; Satyanarayana et al., 2009; Xie et al., 2013) and other biodegradable reinforced films (Behera et al., 2012).

When higher filler contents are used, particle density increases promoting the interaction between filler particles, which could induce the formation of aggregates. The presence of these aggregates together with large size residue particles induces defects in the matrix which affect film structure integrity (Fig. 4d), probably due to their high volume. Ludueña et al. (2012) stressed that the

Table 3
Cassava starch reinforced films properties.

Filler (%)	WVP × 10^{-11} (g/m s Pa)	Humidity (%)	Thickness (μm)	Tensile strength (MPa)	Elongation at break (%)	Toughness (kJ/m^3)	Dynamic elastic modulus (MPa)
0	9.480 ± 1.91[a]	20.08 ± 0.95[c]	48 ± 3[a]	2.03 ± 0.85[a]	248.4 ± 18.8[c]	1553 ± 245[c]	118 ± 44[a]
0.75	13.112 ± 2.12[b]	14.34 ± 0.02[b]	98 ± 20[b]	10.61 ± 0.73[b]	18.9 ± 3.6[b]	1168 ± 261[c]	646 ± 17[b]
1.50	14.612 ± 0.72[b]	12.70 ± 0.03[a]	137 ± 30[b,c]	18.01 ± 0.19[c]	4.4 ± 0.1[a]	361 ± 59[b]	1220 ± 390[c]
3	23.362 ± 1.39[c]	12.16 ± 0.06[a]	172 ± 34[c]	21.92 ± 1.88[d]	4.2 ± 0.7[a]	223 ± 11[a]	1444 ± 409[c]

Note: Reported values correspond to the mean ± standard deviation. Results are expressed on dry basis.
Different letters within the same column indicates significant differences ($p < 0.05$).

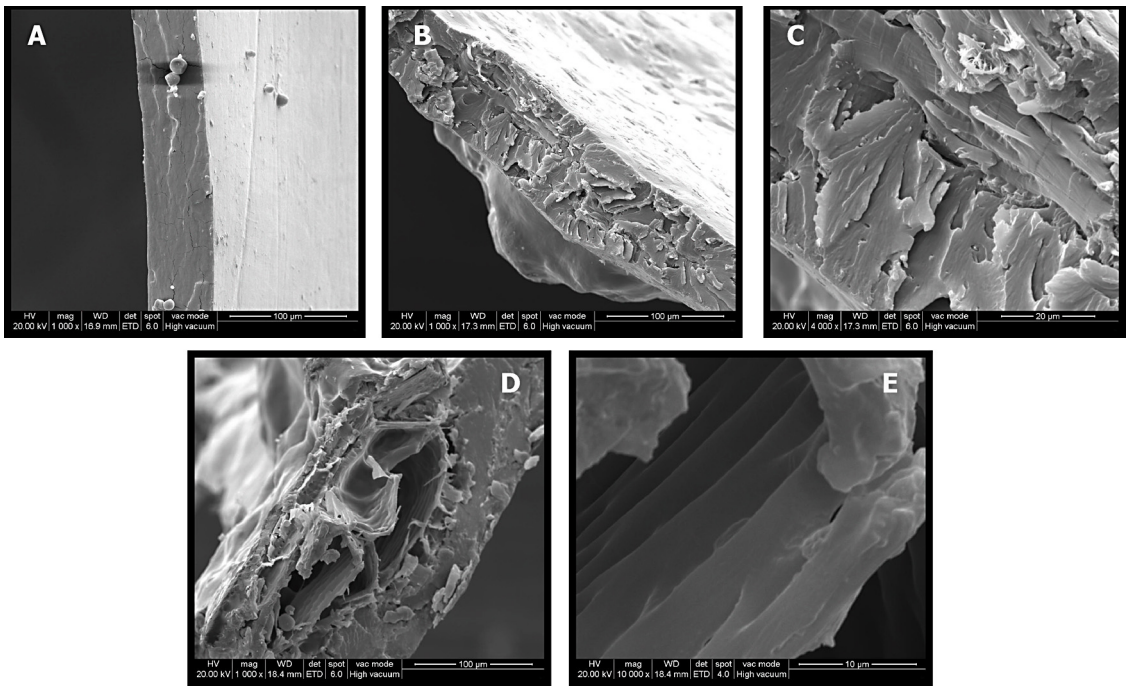

Fig. 4. SEM micrographs of cassava starch films plasticized with 25% w/w glycerol: (a) without filler 1000×; (b) 1.5% w/w filler content 1000×; (c) detail form 1.5% filler content film 10,000×; (d) 3% filler content 1000×; (e) detail from 3% filler content film 10,000×.

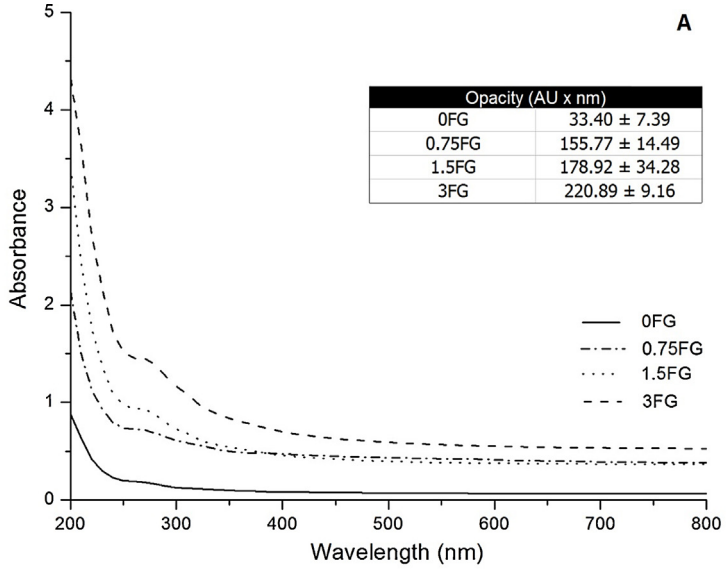

Opacity (AU x nm)	
0FG	33.40 ± 7.39
0.75FG	155.77 ± 14.49
1.5FG	178.92 ± 34.28
3FG	220.89 ± 9.16

Color parameters of cassava films with different fiber content. B

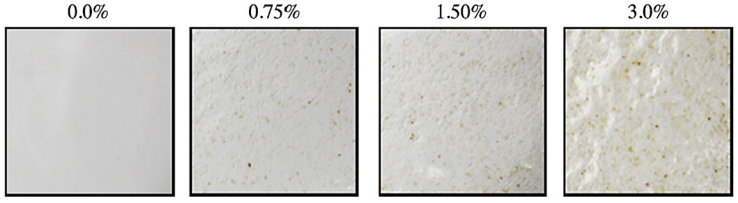

	0.0%	0.75%	1.50%	3.0%
L	95.56[a]	94.56[b]	93.00[c]	90.21[d]
C*	3.30[a]	5.67[b]	7.85[c]	10.42[d]
h°	1.54[a]	-1.54[b]	-1.53[b]	-1.53[b]
ΔE	2.63[a]	4.96[b]	7.59[c]	11.41[d]

Different letters within the same line indicate significant differences ($p<0.05$).

Fig. 5. Optical properties of cassava starch films: (a) UV–Vis light absorption spectrum; (b) photographs of plasticized cassava starch films with different fiber contents and color parameters.

agglomerates do not allow the correct matrix-filler interaction, and therefore weaker polymer-filler interfacial adhesion is observed. Despite the high compatibility of the filler and the matrix, such interactions are present only in the filler particle surface (Fig. 4d).

Fig. 4c and e correspond to a detail of the films cross sections, where certain anatomical elements such as cellular debris, presumably from parenchymal cells, are identified.

Film optical properties are shown in Fig. 5. The study of the UV light absorption capacity of the biodegradable films is relevant to determine their possible applications for packaging. Fig. 5a shows the obtained spectrum and the opacity calculated from absorption spectrum in the visible zone for the studied plasticized films. Reinforced films UV spectra showed a characteristic peak at 250–300 nm, which could be mainly attributed to the phenolic components of lignin (Buranov and Mazza, 2008). In order to estimate the UV-barrier capacity of reinforced films, the area under the curve in the UV region was calculated. As it can be expected, this parameter increased with filler content, being the obtained values: 155.77 ± 14.49, 178.92 ± 34.28 and 220.89 ± 9.16 AU × nm for 0.75, 1.5 and 3%, respectively. A similar trend was observed for opacity in the visible region. Visually films that did not include filler showed higher homogeneity than the reinforced ones, resulting more translucent (Fig. 5b). The effect of filler addition on plasticized films color parameters is shown in the Table inserted in Fig. 5b. Luminosity parameter (L) decreased with filler content while *Chroma* (C^*) and color difference (ΔE) parameter increased. The change in hue angle (h°), however, remained constant regardless of fiber concentration. These results agree with the visual observations previously described (Fig. 5b). Furthermore, it should be noticed that the decrease in luminosity parameter with filler content is in agreement with the opacity increase.

3.4. Water vapor permeability and mechanical properties

Films water vapor permeability was significantly affected ($p < 0.05$) by glycerol and fiber addition. A significant ($p < 0.05$) reduction in WVP values was observed with glycerol addition, depending its optimum concentration on fiber content (Fig. 6). Glycerol interferes with polymeric chain association decreasing the rigidity of the network; thus a less ordered film structure without pores or cracks is obtained, decreasing WVP (López et al., 2008). A similar trend was informed by Galdeano et al. (2009) for oat starch films plasticized with glycerol (20 g/100 g starch). In the case of reinforced films the lower WVP values corresponded to 25% glycerol w/w (Fig. 6a). Nevertheless, the effect of plasticizer on films water vapor barrier properties is less significant than that of the filler (Fig. 6b).

It is well known that water vapor transmission through a material is a balance of three main mechanisms (Ludueña et al., 2012): the film crystallinity, the tortuosity of the pathway, and the presence of surface or structural defects. Although the filler presence increases the tortuosity of the pathway for water molecules, large filler particles promote the generation of voids in the polymer/filler interface as well as surface defects which facilitates the water molecules transport throughout these regions. According to Garcia et al. (2014) WVP decreases in more compact films with a more homogenous structure. Thus, WVP results are in agreement with SEM observations and could be associated to the heterogeneous structure of reinforced matrixes (Fig. 4b and d).

Ludueña et al. (2012) reported that the presence of a natural filler decreased crystallinity degree of the polycaprolactone matrix, thereby increasing the biomaterial permeability to water molecules. However, the effect of fillers on biodegradable matrixes WVP depend on filler type and concentration, polymer structure and their compatibility, which has led to discrepancies on the reported tendencies. In the case of starch films Aila-Suarez et al. (2013) stressed that cotton cellulose addition to potato or chayote tuber starch biocomposites increase water barrier ability. Likewise, Müller et al. (2009) working on cassava starch reinforced films with softwood short fibers reported a similar effect. WVP values for cassava starch films reinforced with the remaining residue of starch extraction are presented in Table 3, showing a decrease in the water barrier ability with filler content. The obtained values are within the range of those of Müller et al. (2009), having in both cases equivalent starch, glycerol and filler contents in film formulations.

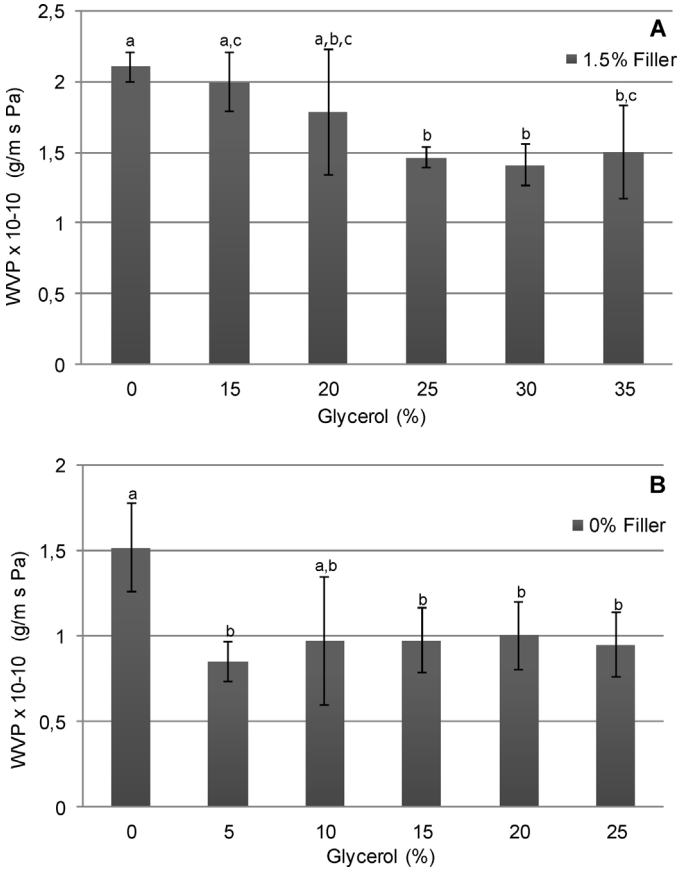

Fig. 6. Plasticizer effect on water vapor permeability of (a) cassava starch based films and (b) films reinforced with 1.5% fiber.

From the mechanical profiles strength to rupture and deformation of the films were obtained, showing both parameters opposite behaviors with the addition of glycerol and filler, as expected (Fig. 7a). Regardless of filler content, films strength decreased significantly ($p < 0.05$) while deformation at break increased with glycerol addition (Fig. 8). This flexibility increase of the material shows the typical effect of plasticizer (Sothornvit and Krochta, 2005) as can be observed in Fig. 8b. For example for 25% glycerol addition films elongation at break increased 4100% with respect to unplasticized ones. When the plasticizer is added the proximity between starch chains were reduced, due to hydrogen bonds formation between hydroxyl groups of plasticizer and those of biopolymer and thus the free volume of film matrix increase (Sothornvit and Krochta, 2005). Under tensile forces, movements of starch chains are facilitated and film flexibility is enhanced. Non-significant differences ($p > 0.05$) were detected in the elongation of reinforced plasticized films for the glycerol concentrations tested. Considering the chemical composition of the residue (Table 2), plasticizer moderated effect in reinforced films could be attributed to glycerol capacity to interact with both lignocellulosic compounds and remaining starch (Averous and Boquillon, 2004).

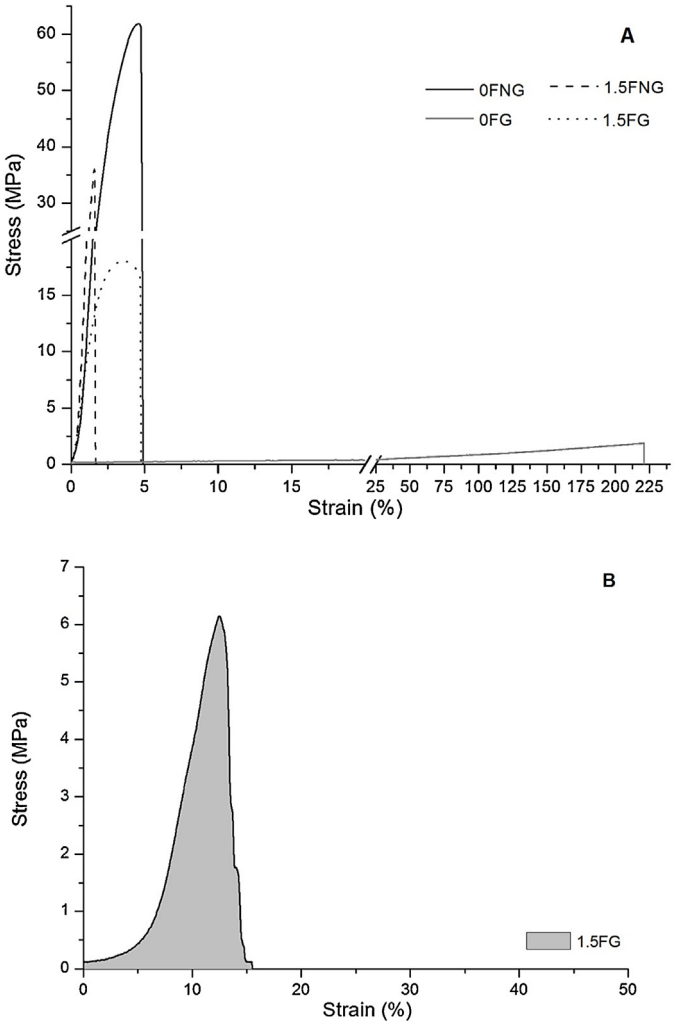

Fig. 7. (a) Stress–strain curves of cassava starch films without plasticizer (0NG), plasticized with 25% w/w glycerol (0G), with 1.5% w/w filler content plasticized (1.5G) and unplasticized (1.5FNG). (b) Stress–strain curves of cassava starch films reinforced zip.

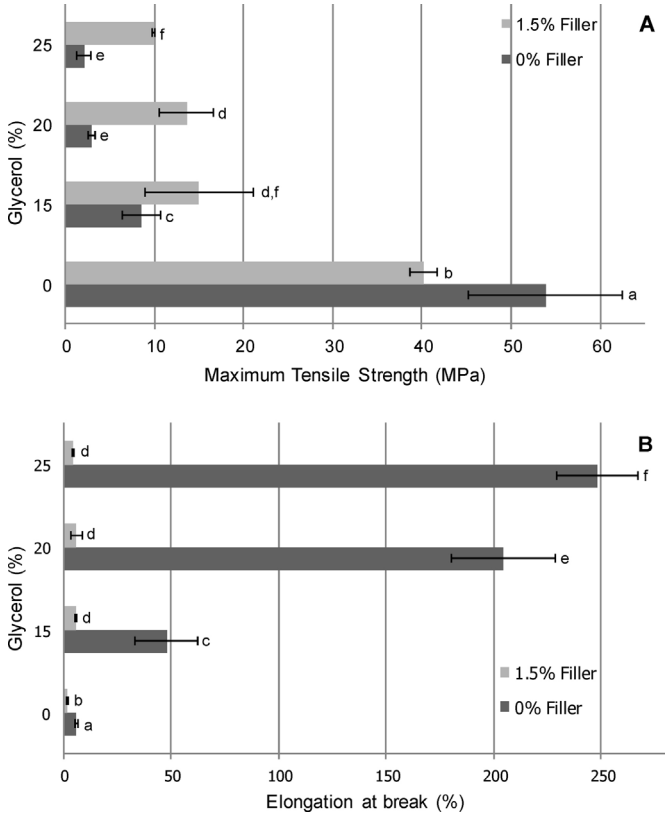

Fig. 8. Plasticizer effect on (a) maximum tensile strength and (b) elongation at break of cassava starch based films and reinforced ones with 1.5% filler.

Moreover, the addition of filler increases film tensile strength confirming the reinforcement of the material (Fig. 8 and Table 3). This is a well-known behavior of polymeric composites reinforced with natural fibers, which has been extensively described by Shalwan and Yousif (2013). However, it was observed that a filler content of 3% led to the formation of more brittle materials, with higher mechanical resistance and elastic modulus, and lower elongation at break and toughness (Table 3). This result is in agreement with SEM observations where the presence of bigger filler particles, which led to a more heterogeneous structure, was detected (Fig. 4d). Besides, maximum resistance of unplasticized films was higher than those with filler due to the stronger chain interactions in starch matrices (Fig. 8a).

Toughness, which represents the total energy absorbed by a material before rupture, comprises the synergic relationship between both tensile strength and elongation. Cassava starch films toughness was $1908 \pm 156\ kJ/m^3$, within the range of that reported by Chang et al. (2006) for tapioca starch films. The addition of 25% glycerol slightly decreased material toughness: $1553 \pm 245\ kJ/m^3$, although differences were not significant ($p > 0.05$). On the other hand, the inclusion of 0.75% filler maintained film toughness (Table 3), while higher filler concentrations decreased significantly ($p < 0.05$) this parameter. Therefore, toughness follows an equivalent behavior than the elongation at break.

DMA assays correlate well with mechanical analysis. Stress–strain curves could be satisfactorily ($r^2 > 0.98$) fitted to the model proposed by Chillo et al. (2008). The values obtained for the elastic modulus of the films with different filler contents are presented in Table 3, showing the same trend as the maximum resistance to rupture.

All films based on cassava starch were sealed by the pulse technique, widely used in the case of flexible synthetic films (Brody and Marsh, 1997). The typical stress–strain curve obtained for cassava starch films with added 1.5% w/w of filler and plasticized with 25% w/w glycerol, is shown in Fig. 7b. Sealed films broke typically near the zip, according to the standard failure mode, indicating the mechanical resistance of the seal.

Compared to synthetic materials, fiber-reinforced films exhibited lower seal strength, since the corresponding values were 4.6 MPa for low density polyethylene (LDPE) and 0.24 MPa for cassava starch reinforced films. Nonetheless, the biodegradable nature of these materials and their ability to be heat sealed, could lead to the development of packaging for specific food applications, such as conservation of organic products.

4. Conclusions

Homogenous biodegradable films can be obtained from cassava starch and the remaining fibrous residue from starch-extraction-process by casting and dehydration method. The residue presented a heterogeneous size distribution, with 44% of the particles bigger than 53 μm. SEM micrographs evidenced that the filler was structurally incorporated in the starch matrix, however with high filler contents a higher contribution of large size fiber particles could be observed.

Reinforced films exhibited UV-barrier capacity, which increases with filler content. Likewise, filler addition increased film opacity while decreased luminosity parameter. Moreover, the obtained materials had good water vapor barrier properties and adequate mechanical strength when 25% w/w glycerol was added as plasticizer. Filler addition reinforced the polymeric matrix increasing its elastic modulus and rupture resistance. On the other hand, toughness followed an equivalent behavior than the elongation at break. The addition of 25% glycerol slightly decreased material toughness while the inclusion of filler contents over 0.75% decreased this parameter.

Considering that the obtained eco-compatible materials can be heat sealed with considerably good seal-strength, their use could be suitable for flexible bags and packaging films manufacture. Furthermore, it should be noted that fibrous residue particles used as fillers in this study were not chemically treated or modified, which would lead to the development of more environmentally friendly and cheaper production process and materials.

In conclusion the addition of natural filler reinforcement constitutes an interesting option to tailor the properties of the resulting composite films, and allows broadening the application range of eco-compatible starch-based materials. Therefore, an integral approach to cassava roots use has been proposed, expanding its scope and providing added value to the remaining residue of starch extraction.

Acknowledgements

The financial support provided by ANPCyT (Project PICT 2011 - 1213) of Argentina is gratefully acknowledged. Authors wish to thank EEA Montecarlo (INTA, Misiones) for cassava roots provision.

References

Abdillahi, H., Chabrat, E., Rouilly, A., Rigal, L., 2013. Influence of citric acid on thermoplastic wheat flour/poly(lactic acid) blends II. Barrier properties and water vapor sorption isotherms. Ind. Crops Prod. 50, 104–111.

Aila-Suarez, S., Palma-Rodriguez, H.M., Rodriguez-Hernandez, A.I., Hernandez-Uribe, J.P., Bello-Perez, L.A., Vargas-Torres, A., 2013. Characterization of films made with chayote tuber and potato starches blending with cellulose nanoparticles. Carbohydr. Polym. 98, 102–107.

Al-Oqla, F.M., Sapuan, S.M., 2014. Natural fiber reinforced polymer composites in industrial applications: feasibility of date palm fibers for sustainable automotive industry. J. Clean. Prod. 66, 347–354.

American Society for Testing and Materials, 1996. Standard test methods for water vapor transmission of materials. ASTM E96/E96M. In: Annual Book of ASTM. ASTM, Philadelphia, PA.

American Society for Testing and Materials, 2000. Standard test method for haze and luminous transmittance of transparent plastics. ASTM D1003-00. In: Annual Book of ASTM. ASTM, Philadelphia, PA.

American Society for Testing and Materials, 2001. Standard test method for seal strength of flexible barrier materials. ASTM F88-00. In: ASTM Standards on Disc. ASTM, Philadelphia, PA.

Association of Official Analytical Chemists, 1997. Total dietary fibre in foods. Enzymatic-gravimetric method. AOAC (985.29). In: Official Methods of Analysis. AOAC, Arlington, VA, USA.

Association of Official Analytical Chemists, 1990. Protein (crude) determination in animal feed: copper catalyst Kjeldahl Method. AOAC (984.13). In: Official Methods of Analysis. AOAC, Arlington, VA, USA.

Averous, L., Boquillon, N., 2004. Biocomposites based on plasticized starch: thermal and mechanical behaviours. Carbohydr. Polym. 56, 111–122.

Behera, A.K., Avancha, S., Basak, R.K., Sen, R., Adhikari, B., 2012. Fabrication and characterizations of biodegradable jute reinforced soy based green composites. Carbohydr. Polym. 88, 329–335.

Bodirlau, R., Teaca, C.-A., Spiridon, I., 2013. Influence of natural fillers on the properties of starch-based biocomposite films. Compos. Part B: Eng. 44, 575–583.

Brody, A., Marsh, K., 1997. The Wiley Encyclopedia of Packaging Technology. John Wiley and Sons, New York.

Buranov, A.U., Mazza, G., 2008. Lignin in straw of herbaceous crops. Ind. Crops Prod. 28, 237–259.

Castaño, J., Rodriguez-Llamazares, S., Carrasco, C., Bouza, R., 2012. Physical, chemical and mechanical properties of pehuen cellulosic husk and its pehuen-starch based composites. Carbohydr. Polym. 90, 1550–1556.

Castillo, L., Lopez, O., Lopez, C., Zaritzky, N., Garcia, M.A., Barbosa, S., Villar, M., 2013. Thermoplastic starch films reinforced with talc nanoparticles. Carbohydr. Polym. 95, 664–674.

Chang, Y.P., Abd Karim, A., Seow, C.C., 2006. Interactive plasticizing–antiplasticizing effects of water and glycerol on the tensile properties of tapioca starch films. Food Hydrocolloids 20, 1–8.

Chillo, S., Flores, S., Mastromatteo, M., Conte, A., Gerschenson, L., Del Nobile, M.A., 2008. Influence of glycerol and chitosan on tapioca starch-based edible film properties. J. Food Eng. 88, 159–168.

Doporto, M.C., Dini, C., Mugridge, A., Viña, S.Z., García, M.A., 2012. Physicochemical, thermal and sorption properties of nutritionally differentiated flours and starches. J. Food Eng. 113, 569–576.

Famá, L., Flores, S., Gerschenson, L., Goyanes, S., 2006. Physical characterization of cassava starch biofilms with special reference to dynamic mechanical properties at low temperatures. Carbohydr. Polym. 66, 8–15.

Famá, L., Goyanes, S., Gerschenson, L., 2007. Influence of storage time at room temperature on the physicochemical properties of cassava starch films. Carbohydr. Polym. 70, 265–273.

Galdeano, M.C., Mali, S., Grossmann, M.V.E., Yamashita, F., García, M.A., 2009. Effects of plasticizers on the properties of oat starch films. Mater. Sci. Eng. C 29, 532–538.

Garcia, P.S., Grossmann, M.V.E., Shirai, M.A., Lazaretti, M.M., Yamashita, F., Muller, C.M.O., Mali, S., 2014. Improving action of citric acid as compatibiliser in starch/polyester blown films. Ind. Crops Prod. 52, 305–312.

Gilfillan, W.N., Nguyen, D.M.T., Sopade, P.A., Doherty, W.O.S., 2012. Preparation and characterisation of composites from starch and sugar cane fibre. Ind. Crops Prod. 40, 45–54.

Guimarães, J.L., Frollini, E., da Silva, C.G., Wypych, F., Satyanarayana, K.G., 2009. Characterization of banana, sugarcane bagasse and sponge gourd fibers of Brazil. Ind. Crops Prod. 30, 407–415.

Han, J.H., Gennadios, A., 2005. Edible films and coatings: a review. In: Han, J.H. (Ed.), Innovations in Food Packaging. Academic Press, London, pp. 239–262, Chapter 15.

Ibrahim, H., Farag, M., Megahed, H., Mehanny, S., 2014. Characteristics of starch-based biodegradable composites reinforced with date palm and flax fibers. Carbohydr. Polym. 101, 11–19.

Konar, S.K., Gu, R., Sain, M., 2013. Preparation and characterization of baked nitrile latex foam reinforced with biomasses. Ind. Crops Prod. 42, 261–267.

Kuciel, S., Liber-Knec, A., 2009. Biocomposites on the base of thermoplastic starch filled by wood and kenaf fiber. J. Biobased Mater. Bioener. 3, 269–274.

Leonel, M., Sarmento, S.B., Cereda, M.P., Cãmara, F.L., 2003. Extração e caracterização de amido de jacatupé (*Pachyrhizus ahipa*). Ciência Tecnol. Alime 23, 362–365.

López, O.V., García, M.A., 2012. Starch films from a novel (*Pachyrhizus ahipa*) and conventional sources: development and characterization. Mater. Sci. Eng. C 32, 1931–1940.

López, O.V., García, M.A., Zaritzky, N.E., 2008. Film forming capacity of chemically modified corn starches. Carbohydr. Polym. 73, 573–581.

López, O.V., Lecot, C.J., Zaritzky, N.E., García, M.A., 2011. Biodegradable packages development from starch based heat sealable films. J. Food Eng. 105, 254–263.

López, O.V., Viña, S.Z., Pachas, A.N.A., Sisterna, M.N., Rohatsch, P.H., Mugridge, A., Fassola, H.E., García, M.A., 2010. Composition and food properties of *Pachyrhizus ahipa* roots and starch. Int. J. Food Sci. Tech. 45, 223–233.

Ludueña, L., Vázquez, A., Alvarez, V., 2012. Effect of lignocellulosic filler type and content on the behavior of polycaprolactone based eco-composites for packaging applications. Carbohydr. Polym. 87, 411–421.

Mali, S., Sakanaka, L.S., Yamashita, F., Grossmann, M.V.E., 2005. Water sorption and mechanical properties of cassava starch films and their relation to plasticizing effect. Carbohydr. Polym. 60, 283–289.

Mancini, M., Moresi, M., Rancini, R., 1999. Mechanical properties of alginate gels: empirical characterisation. J. Food Eng. 39, 369–378.

Müller, C.M.O., Laurindo, J.B., Yamashita, F., 2009. Effect of cellulose fibers addition on the mechanical properties and water vapor barrier of starch-based films. Food Hydrocolloids 23, 1328–1333.

Muscat, D., Adhikari, B., Adhikari, R., Chaudhary, D.S., 2012. Comparative study of film forming behaviour of low and high amylose starches using glycerol and xylitol as plasticizers. J. Food Eng. 109, 189–201.

Perdomo, J., Cova, A., Sandoval, A.J., García, L., Laredo, E., Müller, A.J., 2009. Glass transition temperatures and water sorption isotherms of cassava starch. Carbohydr. Polym. 76, 305–313.

Prakash Maran, J., Sivakumar, V., Sridhar, R., Prince Immanuel, V., 2013. Development of model for mechanical properties of tapioca starch based edible films. Ind. Crops Prod. 42, 159–168.

Rodriguez-Gonzalez, F.J., Ramsay, B.A., Favis, B.D., 2004. Rheological and thermal properties of thermoplastic starch with high glycerol content. Carbohydr. Polym. 58, 139–147.

Satyanarayana, K.G., Arizaga, G.G.C., Wypych, F., 2009. Biodegradable composites based on lignocellulosic fibers: —an overview. Prog. Polym. Sci. 34, 982–1021.

Shalwan, A., Yousif, B.F., 2013. In state of art: Mechanical and tribological behaviour of polymeric composites based on natural fibres. Mater. Des. 48, 14–24.

Sothornvit, R., Krochta, J.M., 2005. Plasticizers in edible films and coatings. In: Han, J.H. (Ed.), Innovations in Food Packaging. Academic Press, London, pp. 403–433, Chapter 23.

Steffe, J.F., 1996. Rheological Methods in Food Process Engineering. Freeman Press, East Lansing, USA.

Technical Association of the Pulp and Paper Industry, 2011. Acid-insoluble lignin in wood and pulp. T222 om-11. In: TAPPI Standards.
United Nations Conference on Trade and Development, http://www.unctad.info/en/Infocomm/AACP-Products/COMMODIRY-PROFILE—Cassava/ 2012. INFOCOMM Commodity Profile: CASSAVA.
Xie, F., Pollet, E., Halley, P.J., Avérous, L., 2013. Starch-based nano-biocomposites. Prog. Polym. Sci. 38, 1590–1628.
Zhang, X., Tong, Q., Zhu, W., Ren, F., 2013. Pasting, rheological properties and gelatinization kinetics of tapioca starch with sucrose or glucose. J. Food Eng. 114, 255–261.